Journal of Materials Chemistry A

PAPER

View Article Online
View Journal

Cite this: DOI: 10.1039/c5ta08209a

Highly efficient and stable quasi-solid-state quantum dot-sensitized solar cells based on a superabsorbent polyelectrolyte†

Wenliang Feng, Yan Li,* Jun Du, Wei Wang and Xinhua Zhong*

Received 13th October 2015
Accepted 22nd December 2015

DOI: 10.1039/c5ta08209a

www.rsc.org/MaterialsA

Limited by the volatilization and leakage of liquid electrolytes, the long-term stability of liquid-junction quantum dot sensitized solar cells (QDSCs) remains a main challenge for the application of QDSCs. Herein, a polyelectrolyte with superior water-absorbing and water-holding capacity, sodium polyacrylate (PAAS), was attempted to gelate conventional aqueous polysulfide electrolytes to construct quasi-solid-state QDSCs. PAAS gel electrolytes have a comparable conductivity with liquid polysulfide electrolytes. Meanwhile, the PAAS gel could penetrate readily into the framework of mesoporous TiO_2 film electrodes due to the strong coordination ability of carboxylate groups on PAAS polymer chains with metal ions. Benefited from the high conductivity of the PAAS gel and its perfect contact with the TiO_2 surface, an impressive photovoltaic performance with a power conversion efficiency of 8.54% in one full sunlight, which is among the best performance for QDSCs, was achieved for CdSeTe QDSCs. Furthermore, the light-soaking stability of the resulting cell devices is significantly improved in comparison with that of the conventional aqueous polysulfide electrolyte based ones.

1. Introduction

Being an alternative light harvesting material to conventional molecular dyes in dye sensitized solar cells (DSCs), colloidal quantum dots (QDs) with the advantageous features of photostability, size dependent optical properties, high molar extinction coefficients and low costs are arousing increasing interest in academic research.[1–6] Benefited from the multiple exciton generation possibility, quantum dot sensitized solar cells (QDSCs) with a theoretical efficiency up to 44% have been considered as one of the promising low-cost third-generation solar cells.[7–12] In recent years, the highest power conversion efficiency (PCE) of QDSCs reported has been continuously renewed.[13–16] By employing a CdSeTe QD sensitizer and an aqueous polysulfide redox electrolyte, a state-of-the-art QDSC has achieved an impressive PCE of 8.55%.[16] However, the long-term performance stability of QDSCs is seriously limited by the volatilization and leakage of liquid electrolytes, which also hampers the durability and large-scale practical application of DSCs.[17–20]

By this consideration, many a research study, based mainly on substituting hole-conducting materials for liquid electrolytes, constructs all-solid-state dye/quantum dot sensitized solar cells.[21–29] Still, the solid-state sensitized solar cells developed face great challenges due to the unsatisfactory conversion efficiency mainly limited by relatively low hole mobility of the hole-transporting material and its inefficient pore filling of the mesoporous TiO_2 film.[21,22,25] To improve the stability and sealing ability of liquid-junction QDSCs and DSCs, an alternative solution, quasi-solid-state solar cells using organic polymer gelators and inorganic gelators, was attempted.[30–48] Unfortunately, the efficiencies of the DSCs or QDSCs with quasi-solid-state electrolytes are often lower than those of liquid electrolyte based solar cells, which can be ascribed to the relatively lower ionic conductivity and imperfect contact with porous TiO_2 film electrodes.[37,39,40] Until now, the highest efficiency of QDSCs with quasi-solid-state electrolytes reported is merely 5.45% under 1 sun irradiation,[46] significantly lower than the corresponding value of the QDSCs with liquid electrolytes.

Polyelectrolytes bearing electrolyte groups are charged polymers, dissociating readily in aqueous solutions and their solution possesses not only the ionic conductivity of electrolytes but also the cohesive property of polymers. As an important class of polyelectrolytes, superabsorbent polyelectrolytes (SBPEs) have been widely used in many applications such as

Key Laboratory for Advanced Materials, Institute of Applied Chemistry, East China University of Science and Technology, Shanghai 200237, China. E-mail: yli@ecust.edu.cn; zhongxh@ecust.edu.cn; Fax: +86 21 6425 0281; Tel: +86 21 6425 0281

† Electronic supplementary information (ESI) available: Conductivity of electrolytes containing different weight ratios of PAAS with a formula weight of 5 000 000 at 25 °C. *J–V* curves of CdSe G-QDSCs based on different weight ratios of PAAS of 30 000 000 formula weight. *J–V* curves of CdSe G-QDSCs based on 15 wt% PAAS of 5 000 000 and 30 000 000 formula weight, respectively, and the relevant photovoltaic parameters. EIS of CdSe based L-QDSCs and G-QDSCs under the forward bias of −0.6 V, and the corresponding simulated values. Normalized V_{oc}, J_{sc} and FF variation of CdSeTe and CdSe based L- and G-QDSCs under successive irradiation provided by using an AM 1.5G solar simulator with an intensity of 100 mW cm^{-2} under room conditions. See DOI: 10.1039/c5ta08209a

fillers in cosmetics, nappies, and drug delivery.[49–51] The superior absorbent ability of SBPEs originates from the electrostatic repulsion between the charges on polymer chains and from the osmotic imbalance between the interior and exterior of gels.[49,53] Even under high centrifugation and mechanical load, it is difficult for swollen SBPEs to lose water interacting strongly with the fixed ions in the network. With the advantages of super water absorbing capacity and excellent water-holding capability in addition to high ionic conductivity, SBPEs are supposed to have potential application in quasi-solid-state solar cells. However, the development of QDSCs and DSCs based on SBPEs has rarely been touched in the literature.

Herein, a photochemically and thermally stable polyelectrolyte with perfect mechanical strength, sodium polyacrylate (PAAS),[49] was used to solidify aqueous polysulfide electrolytes to prepare quasi-solid-state gel electrolytes for QDSCs. PAAS is a typical negatively charged polyelectrolyte with hydrophilic groups and a three-dimensional network, by which a large quantity of water can be rapidly absorbed into the framework of PAAS.[49–53] More importantly, PAAS bearing carboxylate groups on the polymer chains exhibits strong capability to coordinate with metal ions.[52] With sufficient water trapped in the framework and the strong interaction between carboxylic groups and metal ions, PAAS is expected to exhibit high ionic conductivity and superior contact with the surface of the mesoporous TiO_2 film.[52,53] Experimental results show that the ionic conductivity of the PAAS based gel electrolyte is comparable to that of aqueous polysulfide electrolyte solutions. Compared with the corresponding QDSCs based on conventional liquid polysulfide electrolytes (L-QDSCs), the PAAS gel based QDSCs (G-QDSCs) present a similar PCE but better stability. Notably, a conversion efficiency as high as 8.54% under one full sunlight was obtained for the QDSCs by using a CdSeTe QD sensitizer, which is the best PCE of the quasi-solid-state QDSCs reported so far.

2. Experimental section

Chemicals

Oleic acid (90%), 3-mercaptopropionic acid (MPA, 98%) and thioglycolic acid (TGA, 97%) were obtained from Alfa Aesar. Oleylamine (OAm, 95%), 1-octadecene (ODE, 90%), tri-octylphosphine (TOP, 90%), cadmium oxide (CdO, 99.99%), selenium powder (200 mesh, 99.99%) and tellurium powder (200 mesh, 99.99%) were purchased from Aldrich. Paraffin liquid (chemical grade) and sodium polyacrylate (PAAS) with an average molecular weight of 5 000 000 and 30 000 000 were received from Shanghai Chemical Reagents Company. All reagents were used without any treatment.

Synthesis of oil-soluble CdSe and $CdSe_{0.65}Te_{0.35}$ QDs

A literature method was adopted with minor modification to synthesize the initial oil-soluble OAm-capped CdSe QDs.[54] Typically, 0.4 mL of 1.0 M Se precursor solution prepared by dissolving Se powder into TOP was mixed with 0.6 mL of TOP and 10.0 mL of OAm. Under the protection of N_2, the above solution was heated to 275 °C followed by injection of 1.0 mL of 0.4 M Cd stock solution obtained by dissolving CdO in oleic acid and ODE (v/v, 1 : 1) at 250 °C. The reaction temperature was kept at 285 °C for 10 min. The oil-soluble CdSe QDs with a particle size of 5.4 ± 0.4 nm were prepared. The first excitonic absorption peak of the obtained CdSe QDs is at about 620 nm. The CdSe QDs were then purified by centrifugation and decantation with the addition of methanol, and finally dispersed in 30 mL of dichloromethane.

Following our previous method, the $CdSe_{0.65}Te_{0.35}$ (CdSeTe) QDs were synthesized by a one-pot procedure that involved directly heating the mixed solution containing Cd, Se, and Te precursors to a desired temperature.[55] Briefly, Te and Se precursor solutions of 0.1 M were prepared by dissolving Se and Te powder in TOP and paraffin liquid (v/v, 1 : 3), respectively, while Cd stock solution of 0.1 M was obtained by dissolving CdO in oleic acid and paraffin liquid (v/v, 1 : 3). The above Cd, Te and Se precursor solutions were loaded in a three-neck flask with a Cd : Te : Se volume ratio of 10 : 1 : 1 and then heated to 320 °C under a N_2 atmosphere. After keeping for 10 min, the reaction temperature was lowered to 260 °C followed by the addition of 2.0 mL of OAm. After reacting for 8 min at 260 °C, the oil-soluble CdSeTe QDs with a particle size of 5.2 ± 0.4 nm and the absorption edge at 800 nm were obtained. Finally, the obtained oil-soluble CdSeTe QDs were purified following the same procedure of CdSe QDs as described above and then dispersed in 30 mL of dichloromethane.

Preparation of water-soluble CdSe and CdSeTe QDs

The hydrophilic QDs were obtained *via* the ligand exchange method reported in the literature.[14,56,57] Generally, 2.0 mmol of MPA was dissolved in 1.0 mL of methanol. The pH value of the solution was adjusted to 10.0 by using 30% NaOH. The above MPA-methanol solution was added into 30 mL of CdSe QD dichloromethane solution at room temperature under stirring. After stirring for 2 h, 20 mL of deionized water was poured into the above solution to displace the hydrophilic CdSe QDs. The water-soluble CdSe QDs capped with MPA were obtained following purification by centrifugation and decantation with acetone. For further use, the obtained CdSe QDs were dissolved in 2.0 mL of deionized water, the pH value of which was adjusted to 10 by adding 10% NaOH. The water-soluble CdSeTe QDs capped by TGA were obtained by the similar method for the preparation of water-soluble CdSe QDs by replacing MPA with TGA.

Fabrication of solar cells

TiO_2 mesoporous film electrodes were prepared by successively screen-printing a transparent layer (9.0 ± 0.5 μm) and a light scattering layer (6.0 ± 0.5 μm) on FTO (8 Ω per square).[58] The QD sensitizers were absorbed on the TiO_2 mesoporous films by dropping 45 μL of MPA-capped water-soluble CdSe QDs or TGA-capped water-soluble CdSeTe QDs onto the TiO_2 mesoporous film and allowing it to stand for 2 h. Then the above electrodes were coated with 4 ZnS layers by dipping the electrodes alternately into 0.1 M $Zn(OAc)_2$ methanol solution and 0.1 M Na_2S aqueous solution for 1 min per dip. The ZnS-coated electrodes

were immersed into the solution (including 100 μL of TEOS, 45 μL of ammonium hydroxide, 2.0 mL of deionized water and 8.0 mL of ethanol) to form a SiO_2 layer.[59]

The $Cu_{2-x}S$/FTO counter electrode (CE) was prepared by screen-printing the pre-prepared $Cu_{2-x}S$ nanoparticles on FTO according to the literature method.[60] The polysulfide electrolyte (2.0 M Na_2S and S aqueous solution) was first obtained by dissolving $Na_2S \cdot 9H_2O$ (4.8 g) and S (0.64 g) in 10 mL of deionized water under ultrasonication. The gel electrolyte was prepared by gradually adding a certain amount of PAAS into the above 10 mL polysulfide electrolyte under stirring at room temperature for 10 min. The gel electrolyte was coated on the CE with a pre-drilled hole. A surlyn ring (DuPont) of 60 μm thickness was used to seal QD-sensitized TiO_2 photoanodes and the $Cu_{2-x}S$/FTO CE. The hole was then sealed with adhesive. For comparison, the liquid QDSCs were constructed by injecting the polysulfide electrolyte into the cells *via* pre-drilled holes on the CE.

Characterization

The UV/vis absorption spectra and PL emission spectra were obtained using a UV-visible spectrophotometer (Shimadzu UV-3101 PC) and a fluorescence spectrophotometer (Cary Eclipse Varian), respectively. The conductivity of the electrolytes was measured by using a DDSJ-308A conductivity meter (Shanghai electronics science instrument Co., Ltd). Current–voltage curves (*J–V* curves) of the cells were measured using a Keithley 2400 source meter under illumination of simulated AM 1.5G solar light (Oriel, model no. 94022A) with an intensity of 100 mW cm^{-2} (1 full sun). The photoactive area was 0.235 cm^2 as defined by a black plastic disk. The incident photon-to-current conversion efficiency (IPCE) spectrum was tested using a Keithley 2000 multimeter under the illumination of a DK240 monochromator with a 300 W tungsten lamp. Electrochemical impedance spectroscopy (EIS) was carried out on an electrochemical workstation (Zahner, Zennium). EIS was performed under dark conditions at different forward bias ranging from 0 V to 0.65 V, applying a 20 mV AC sinusoidal signal over the constant applied bias with the frequency ranging from 1 MHz to 0.1 Hz.

3. Results and discussion

Ionic conductivity of the PAAS gel electrolyte

In sensitized solar cells, electrolytes are the hole-transport mediators, responsible for the charge carrier transport and the regeneration of the sensitizer *via* redox couple transportation between the photoanode and cathode. The transport ability can be mainly reflected by ion conductivity and diffusivity of the electrolyte, the issues directly affecting the efficient generation of electricity. The conductivity (σ) of an electrolyte is related to the diffusion coefficient (D_i) and can be described by the following equation.[61]

$$\sigma(T) = \sum_i |z_i| F c_i \mu_i = \sum_i \frac{|z_i|^2 F c_i e D_i}{K_B T} \quad (1)$$

where z_i, c_i and D_i are the charge, concentration and diffusion coefficient of the conducting ions, and T, K_B and F are the absolute temperature, Boltzmann and Faraday constants, respectively.

To explore the effect of gelation of polysulfide solution on the electrolyte performance, the conductivity of both liquid and gel electrolytes was examined. The conductivity of electrolytes containing various weight ratios of PAAS with a formula weight of 30 000 000 at room temperature (25 °C) is shown in Fig. 1a. The gel electrolytes with the PAAS under 15 wt% exhibit a relatively high conductivity at room temperature, though the gelation caused a slight decrease of ionic conductivity. The gel electrolyte with 15 wt% PAAS presents a conductivity of up to 80.4 mS cm^{-1}, just 6.7% lower than that of the liquid polysulfide electrolyte (86.2 mS cm^{-1}). The high conductivity should be due to the three-dimensional porous structure of PAAS that provides a channel for the free migration of ions. When the amount of PAAS reached 20 wt%, an obvious decrease of conductivity was observed, which may be ascribed to the reduction of free volume ratio of polysulfide solution in the gel electrolyte.[62]

From eqn (1), the conductivity is also related to temperature. Generally, when an ionic transport process involves an

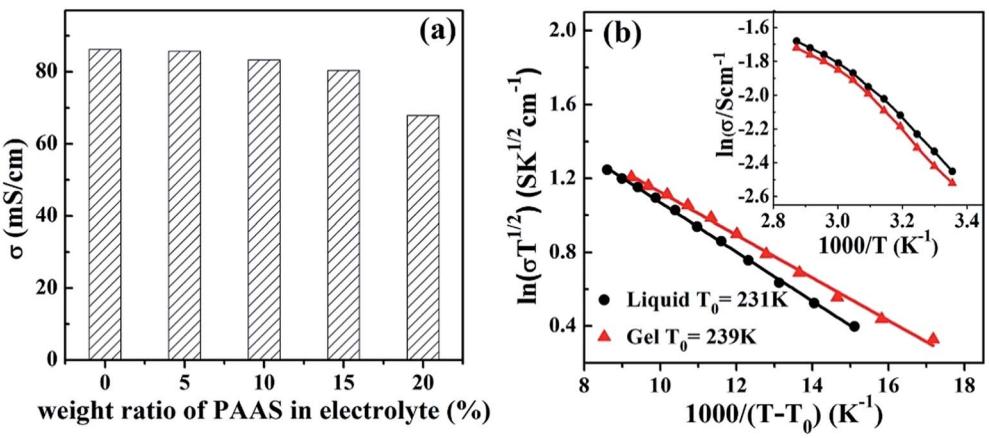

Fig. 1 (a) Conductivity of electrolytes containing different weight ratios of PAAS with a formula weight of 30 000 000 at 25 °C. (b) Temperature-dependent conductivity of the liquid and gel electrolytes based on 15 wt% PAAS in the VTF type. Inset: Arrhenius plots of conductivity-temperature data.

intermolecular ion hopping, the conductivity will be determined by the thermal hopping frequency and the conductivity-temperature behavior can be described by the Arrhenius equation (eqn (2)),[61] in which the conductivity *versus* $\exp(-E/kT)$ is linear.

$$\sigma = A \exp(-E_a/kT) \quad (2)$$

where σ is the ionic conductivity, A is a constant, T is the absolute temperature, and E_a is the activation energy. When the ion transport is dominated by the mobility of the solvent molecules, the conductivity will rely on the free volume of the solvent and the conductivity-temperature characteristics can be described by the Vogel–Tammann–Fulcher (VTF) equation (eqn (3))[62]

$$\sigma(T) = AT^{-1/2} \exp[-E_a(T - T_0)] \quad (3)$$

where σ is the specific conductivity, A is a pre-exponential factor proportional to $T^{1/2}$, T is the absolute temperature, E_a is the activation energy, and T_0 is the glass-transition temperature. To illustrate the ion–solvent interactions in the electrolyte, the dependence of conductivity on temperature was explored. As can be seen from the inset of Fig. 1b, the plots are obviously not linear. Therefore, the Arrhenius equation cannot be used to describe the conductivity-temperature behavior of both liquid polysulfide and PAAS gel electrolytes. Based on the VTF equation, the plots extremely coincide with the VTF-type (Fig. 1b), and the fitted VTF parameters are listed in Table 1. This indicates that the conductivity of the above electrolytes is mainly determined by the motion of ions.[39]

Table 1 Parameters of the electrolytes fitted by the VTF type

The electrolytes	$\ln A$ (S cm^{-1}) $(T/K)^{1/2}$	T_0 (K)	E_a (kJ mol^{-1})
Liquid	2.41	231.96	134.52
Gel	2.29	239.93	117.78

Photovoltaic performance of quasi-solid-state QDSCs

In order to reflect the effect of gelation on the photovoltaic performance of the cell devices, the *J–V* curve measurements of both G-QDSCs and corresponding L-QDSCs using CdSeTe QDs as sensitizers were conducted and are shown in Fig. 2. The relevant photovoltaic parameters of both average and champion values are presented in Table 2. From Fig. 2a and Table 2, it can be observed that the open-circuit voltages (V_{oc}) and fill factors (FF) of G-QDSCs with the PAAS concentration under 15 wt% are slightly higher than those of L-QDSCs, while the short-circuit current density (J_{sc}) shows a slight decrease with gelation of the electrolyte. The slight enhancement of V_{oc} can be attributed to the reduction of charge recombination between the photoanode and electrolyte. Due to the strong capability to interact with TiO_2 nanoparticles, PAAS could provide a protective layer over both TiO_2 and QD surfaces by the steric hindrance effect, consequently retarding the unwanted charge recombination between the photoanode and the electrolyte and enhancing the V_{oc}. Meanwhile, by the strong coordination ability of carboxylate groups with metal ions, the PAAS gel could permeate readily into the framework of mesoporous TiO_2 films and exhibit superior contact with the TiO_2 surface, leading to the slight improvement of the fill factor (FF). Notably, the high ionic conductivity of the gel electrolyte with a PAAS concentration under 15 wt% avoids the significant decline of the J_{sc}, and the overall conversion efficiencies of G-QDSCs are similar to that of L-QDSCs. When the weight ratio of PAAS reaches 20 wt% in the gel electrolyte, all photovoltaic parameters, V_{oc}, J_{sc} and FF, are obviously reduced, consequently giving rise to the relatively low PCE. The reduced photovoltaic performance could be derived from the low ionic conductivity of the gel electrolyte with 20 wt% PAAS. By consideration of the high conductivity and appropriate viscosity of electrolytes in addition to high PCE of the cells developed, the gel electrolyte with a PAAS of 15 wt% was considered to be the optimized concentration to construct G-QDSCs.

To verify the influence of formula weight of PAAS on the cell performance, the *J–V* curves of the G-QDSCs based on PAAS with

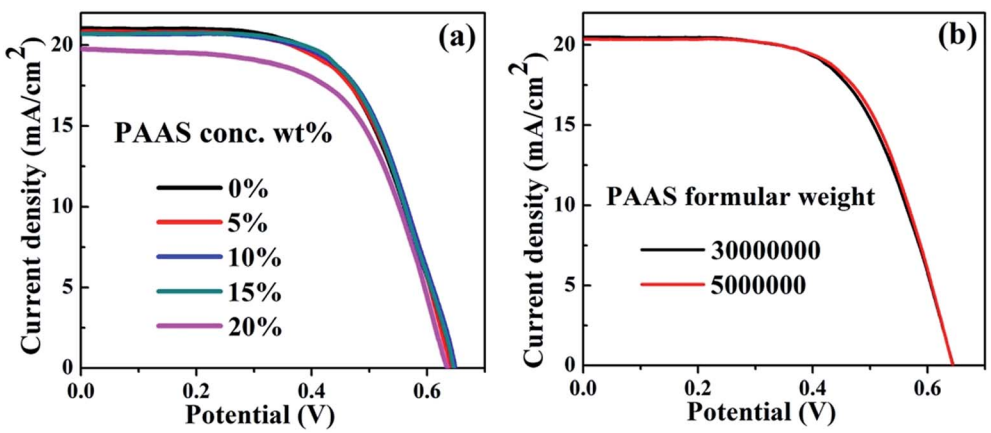

Fig. 2 (a) *J–V* curves of CdSeTe sensitized solar cells based on the polysulfide electrolyte containing different weight ratios of PAAS with a formula weight of 30 000 000. (b) *J–V* curves of CdSeTe sensitized solar cells based on gel electrolytes with 15 wt% PAAS of 5 000 000 and 30 000 000 formula weight.

Table 2 Photovoltaic parameters of CdSeTe sensitized solar cells based on electrolytes containing different weight ratios of PAAS with 30 000 000 formula weight[a]

PAAS (wt%)	J_{sc} (mA cm^{-2})	V_{oc} (V)	FF (%)	PCE (%)
Liquid	20.98(21.08)	0.655(0.657)	61.45(61.83)	8.44 ± 0.04(8.56)
5%	20.83(20.85)	0.658(0.661)	61.89(61.95)	8.48 ± 0.07(8.54)
10%	20.65(20.71)	0.660(0.663)	62.22(62.41)	8.48 ± 0.05(8.57)
15%	20.49(20.57)	0.662(0.664)	62.40(62.55)	8.46 ± 0.03(8.54)
20%	19.86(20.02)	0.645(0.651)	60.93(61.17)	7.80 ± 0.04(7.97)

[a] Average parameters and standard deviation based on 5 solar cells in parallel. The numbers in parentheses represent the values obtained for the champion cells.

Table 3 Photovoltaic parameters of CdSeTe sensitized solar cells based on gel electrolytes with 15 wt% PAAS of 5 000 000 and 30 000 000 formula weight[a]

PAAS (Fw)	J_{sc} (mA cm^{-2})	V_{oc} (V)	FF (%)	PCE (%)
30 000 000	20.49(20.57)	0.662(0.664)	62.40(62.55)	8.46 ± 0.03(8.54)
5 000 000	20.56(20.63)	0.659(0.664)	62.29(62.49)	8.44 ± 0.09(8.56)

[a] Average parameters and standard deviation based on 5 solar cells in parallel. The numbers in parentheses represent the values obtained for the champion cells.

different formula weights are shown in Fig. 2b. It can be clearly seen that there is no remarkable difference between the two curves (Table 3), which is consistent with the similar conductivity of both gel electrolytes shown in Fig. S1.† Thus, the PAAS with a wide range of formula weights can be used to construct the quasi-solid-state QDSCs. In this paper, we chose PAAS of 30 000 000 formula weight as a model gelator to prepare the gel electrolyte and fabricate G-QDSCs.

Electrochemical impedance spectroscopy (EIS)

For further illuminating the effect of gelation on the performance of QDSCs, electrochemical impedance spectroscopy (EIS) was carried out. Both gel and liquid electrolyte based QDSCs were measured in the dark under different forward bias, applying a 20 mV AC sinusoidal signal over the constant applied bias with the frequency ranging between 1 MHz and 0.1 Hz. Generally, there are two semicircles in Nyquist plots: a very small semicircle in the high-frequency region (reflecting charge transfer resistance at the counter electrode/electrolyte interface), and a large semicircle in the middle- and low-frequency region (reflecting the recombination at the photoanode/electrolyte interface). The experimental data were fitted by the equivalent circuit as shown in Fig. 3c (the inset). The fitted results of the C_{μ} (chemical capacitance standing for the change of electron density as a function of the Fermi level) and R_{rec} (the charge recombination resistance at the photoanode/electrolyte interfaces)[63] are shown in Fig. 3a and b. The similar C_{μ} values of both cells demonstrate that gelation of the liquid polysulfide electrolyte does not affect the level of the conduction band or the density of states of TiO_2. Notably, after the gelation by PAAS, the R_{rec} values, inverse to electron recombination rate between TiO_2/QDs/electrolyte interfaces,[63] slightly increased. The results illustrate that the application of the gel electrolyte is favorable for the reduction of charge recombination between TiO_2/QDs/electrolyte interfaces, consequently giving rise to the slight enhancement of V_{oc} as discussed above. For intuition, the Nyquist plots for the cells based on both gel and liquid electrolytes at a forward bias of −0.65 V are shown in Fig. 3c, and the relevant EIS parameters are listed in Table 4. From Table 4, the G-QDSCs and L-QDSCs present the similar R_s (the series resistance) and R_{CE} (the charge transfer resistance at the counter-electrode/electrolyte interface),[63] indicating that the gelation of the electrolyte by PAAS has no negative effects on the charge transfer between the interfaces of the electrode/electrolyte and TiO_2/QDs/electrolyte.

Table 4 Simulated values of resistance (R) and capacitance (C) under the forward bias of −0.65 V of CdSeTe sensitized L- and G-QDSCs

The cells	R_s (Ω cm^2)	R_{CE} (Ω cm^2)	R_{rec} (Ω cm^2)	C_{μ} (mF cm^{-2})	τ_n (ms)
L-QDSCs	23.15	5.16	223	8.2	1828.6
G-QDSCs	22.89	5.41	252	7.9	1990.8

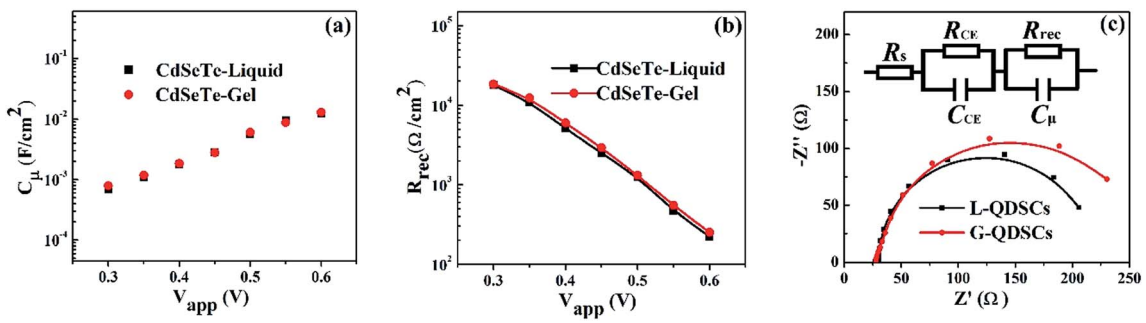

Fig. 3 EIS of CdSeTe sensitized L-QDSCs and G-QDSCs: (a) chemical capacitance C_{μ}; (b) recombination resistance R_{rec}; (c) Nyquist plots at −0.65 V forward bias (inset: the equivalent circuit used to fit EIS).

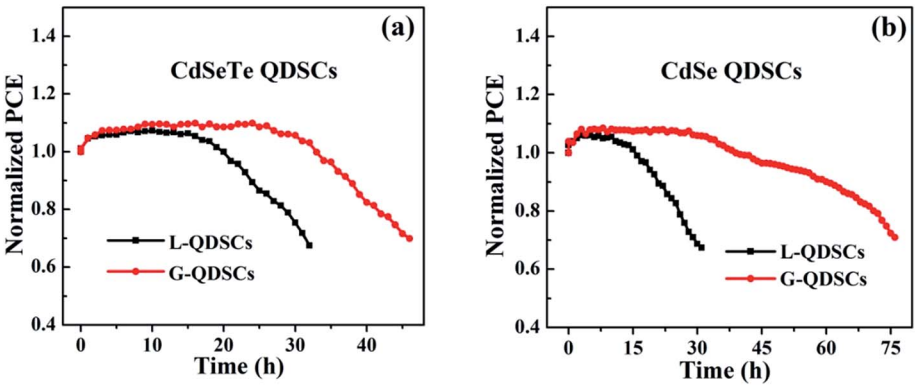

Fig. 4 Normalized performance variation of L-QDSCs and G-QDSCs under successive irradiation provided by using an AM 1.5G solar simulator with an intensity of 100 mW cm^{-2} under room conditions: (a) CdSeTe sensitized QDSCs; (b) CdSe sensitized QDSCs.

In this study, CdSe based G-QDSCs were also constructed to further verify the effect of the PAAS gel on the performance of QDSCs. The experimental data show that the CdSe based G-QDSCs also exhibit comparable PCE with that of L-QDSCs (Fig. S2 and S3, Table S1, S2 and S3†). The results indicate that the prepared gel electrolyte is suitable for different types of QD sensitizers to fabricate quasi-solid-state QDSCs.

Stability of quasi-solid-state QDSCs

Stability is one of the most important issues concerning solar cells. In order to evaluate the stability of PAAS gel electrolytes fabricated in QDSCs, both CdSeTe and CdSe sensitized G-QDSCs were sealed and tested under successive irradiation by using an AM 1.5G solar simulator with an intensity of 100 mW cm^{-2} at room temperature. For comparison, the stability of corresponding L-QDSCs was also examined under the same conditions.

As shown in Fig. 4a, the PCE of both CdSeTe based L- and G-QDSCs increased rapidly in the first 2 h, which is commonly observed in sensitized solar cells and should derive from the requirement time for electrolytes to permeate into the mesoporous TiO_2 film. Under 25 h successive irradiation, the PCE of quasi-solid-state QDSCs shows no obvious decrease. 69% of its initial efficiency is retained with a further extension of irradiation time to 46 h. On the contrary, only after 32 h irradiation the PCE of the QDSCs based on liquid electrolytes decreases significantly by 33%, which can be attributed mainly to the reduction of J_{sc} by nearly 30% (Fig. S4†). As can been seen from Fig. 4b, the stability of the liquid-junction QDSCs based on CdSe QDs is effectively enhanced by gel electrolytes. The efficiency of L-QDSCs started to decline after 12 h successive irradiation, and only 68% of its initial efficiency was conserved after 31 h irradiation. By contrast, the G-QDSCs might maintain the best efficiency for nearly 30 h, keeping up to 70% of its initial efficiency after 77 h successive irradiation. The results showed that the gelation of liquid polysulfide using PAAS obviously improved the stability of QDSCs, which could be due to both the intrinsic protection of the PAAS framework for polysulfide oxidation and the retardation of the permeation of the electrolyte from the sealed QDSC devices.

4. Conclusions

In summary, a novel polyelectrolyte gel was prepared by simply mixing PAAS and polysulfide aqueous solution. The ionic conductivity measurements demonstrate that the PAAS gel electrolyte exhibits high conductivity, comparable to that of liquid polysulfide electrolyte solution. It should be ascribed to the superabsorbent ability of PAAS by swelling of the three dimensional porous network that could provide a channel for ion mobility. Both CdSeTe and CdSe QDs were used as models to construct quasi-solid-state QDSCs based on the PAAS gel. Benefited from the high ionic conductivity of the PAAS gel and its good perfect contact with the TiO_2 surface, both CdSeTe and CdSe based quasi-solid-state QDSCs exhibit comparable PCE with that of reference liquid-junction QDSCs. Notably, by combination with CdSeTe QD sensitizers, an unprecedented PCE of 8.54% for gel-QDSCs was obtained. Moreover, the light-soaking stability of the cell devices based on both CdSeTe and CdSe QD sensitizers was significantly improved, which could be attributed to the water-holding capacity of PAAS that could prevent the volatilization and leakage of liquid electrolytes. The application of superabsorbent polyelectrolytes in gel electrolytes provides a new approach for the construction of quasi-solid-state QDSCs.

Acknowledgements

We acknowledge the National Natural Science Foundation of China (No. 21421004, 91433106, and 21301059), the Open Project of State Key Laboratory of Chemical Engineering (SKL-ChE-14C04), and the Fundamental Research Funds for the Central Universities in China for financial support.

References

1 A. J. Nozik, M. C. Beard, J. M. Luther, M. Law, R. J. Ellingson and J. C. Johnson, *Chem. Rev.*, 2010, **110**, 6873–6890.
2 O. E. Semonin, J. M. Luther, S. Choi, H.-Y. Chen, J. Gao, A. J. Nozik and M. C. Beard, *Science*, 2011, **334**, 1530–1533.

3 J. R. Swierk and T. E. Mallouk, *Chem. Soc. Rev.*, 2013, **42**, 2357–2387.
4 J. B. Sambur, T. Novet and B. A. Parkinson, *Science*, 2010, **330**, 63–66.
5 E. H. Sargent, *Nat. Photonics*, 2012, **6**, 133–135.
6 S. Ruhle, M. Shalom and M. Zaban, *ChemPhysChem*, 2010, **11**, 2290–2304.
7 P. V. Kamat, K. Tvrdy, D. R. Baker and J. G. Radich, *Chem. Rev.*, 2010, **110**, 6664–6688.
8 P. V. Kamat, *Acc. Chem. Res.*, 2012, **45**, 1906–1915.
9 Z. Yang, C.-Y. Chen, C.-W. Liu and H.-T. Chang, *Chem. Commun.*, 2010, **46**, 5485–5487.
10 I. Mora-Sero and J. Bisquert, *J. Phys. Chem. Lett.*, 2010, **1**, 3046–3052.
11 I. J. Kramer and E. H. Sargent, *Chem. Rev.*, 2014, **114**, 863–882.
12 C. M. Chuang, P. R. Brown, V. Bulovic and M. G. Bawendi, *Nat. Mater.*, 2014, **13**, 796–801.
13 J. Wang, I. Mora-Seró, Z. Pan, K. Zhao, H. Zhang, Y. Feng, G. Yang, X. Zhong and J. Bisquert, *J. Am. Chem. Soc.*, 2013, **135**, 15913–15922.
14 Z. Pan, I. Mora-Seró, Q. Shen, H. Zhang, Y. Li, K. Zhao, J. Wang, X. Zhong and J. Bisquert, *J. Am. Chem. Soc.*, 2014, **136**, 9203–9210.
15 S. Jiao, Q. Shen, I. Mora-Seró, J. Wang, Z. Pan, K. Zhao, Y. Kuga, X. Zhong and J. Bisquert, *ACS Nano*, 2015, **9**, 908–915.
16 K. Zhao, Z. Pan, I. Mora-Seró, E. Canovas, H. Wang, Y. Song, X. Gong, J. Wang, M. Bonn, J. Bisquert and X. Zhong, *J. Am. Chem. Soc.*, 2015, **137**, 5602–5609.
17 P. Wang, S. M. Zakeeruddin, P. Comte, I. Exnar and M. Grätzel, *J. Am. Chem. Soc.*, 2003, **125**, 1166–1167.
18 J. Wu, Z. Lan, J. Lin, M. Huang, Y. Huang, L. Fan and G. Luo, *Chem. Rev.*, 2015, **115**, 2136–2173.
19 A. Hagfeldt, G. Boschloo, L. Sun, L. Kloo and H. Pettersson, *Chem. Rev.*, 2010, **110**, 6595–6663.
20 J. Du, X. Meng, K. Zhao, Y. Li and X. Zhong, *J. Mater. Chem. A*, 2015, **3**, 17091–17097.
21 E. Kinder, P. Moroz, G. Diederich, A. Johnson, M. Kirsanova, A. Nemchinov, T. O'Connor, D. Roth and M. Zamkov, *J. Am. Chem. Soc.*, 2011, **133**, 20488–20499.
22 H. Wang, J. Li, F. Gong, G. Zhou and Z.-S. Wang, *J. Am. Chem. Soc.*, 2013, **135**, 12627–12633.
23 B. Lee, C. C. Stoumpos, N. Zhou, F. Hao, C. Malliakas, C.-Y. Yeh, T. J. Marks, M. G. Kanatzidis and R. P. H. Chang, *J. Am. Chem. Soc.*, 2014, **136**, 15379–15385.
24 S. Ma, M. Shang, L. Yu and L. Dong, *J. Mater. Chem. A*, 2015, **3**, 1222–1229.
25 I. Chung, B. Lee, J. He, R. P. H. Chang and M. G. Kanatzidis, *Nature*, 2012, **485**, 486–489.
26 C. T. Weisspfennig, M. M. Lee, J. Teuscher, P. Docampo, S. D. Stranks, H. J. Joyce, H. Bergmann, I. Bruder, D. V. Kondratuk, M. B. Johnston, H. J. Snaith and L. M. Herz, *J. Phys. Chem. C*, 2013, **117**, 19850–19858.
27 S. Inudo, M. Miyake and T. Hirato, *Phys. Status Solidi A*, 2013, **210**, 2395–2398.
28 Y. Oda, H. Shen, L. Zhao, J. Li, M. Iwamoto and H. Lin, *Sci. Technol. Adv. Mater.*, 2014, **15**, 035006.
29 M. Planells, A. Abate, D. J. Hollman, S. D. Stranks, V. Bharti, J. Gaur, D. Mohanty, S. Chand, H. J. Snaith and N. Robertson, *J. Mater. Chem. A*, 2013, **1**, 6949–6960.
30 L. Tao, Z. Huo, Y. Ding, Y. Li, S. Dai, L. Wang, J. Zhu, X. Pan, B. Zhang, J. Yao, M. K. Nazeeruddin and M. Grätzel, *J. Mater. Chem. A*, 2015, **3**, 2344–2352.
31 P. Wang, S. M. Zakeeruddin, J. E. Moser, M. K. Nazeeruddin, T. Sekiguchi and M. Grätzel, *Nat. Mater.*, 2003, **2**, 402–407.
32 N. Mohmeyer, P. Wang, H.-W. Schmidt, S. M. Zakeeruddin and M. Grätzel, *J. Mater. Chem.*, 2004, **14**, 1905–1909.
33 L. Wang, S. Fang, Y. Lin, X. Zhou and M. Li, *Chem. Commun.*, 2005, **45**, 5687–5689.
34 Y. Shi, C. Zhan, L. Wang, B. Ma, R. Gao, Y. Zhu and Y. Qiu, *Phys. Chem. Chem. Phys.*, 2009, **11**, 4230–4235.
35 C.-H. Yang, W.-Y. Ho, H.-H. Yang and M.-L. Hsueh, *J. Mater. Chem.*, 2010, **20**, 6080–6085.
36 K. S. Lee, Y. Jun and J. H. Park, *Nano Lett.*, 2012, **12**, 2233–2237.
37 Q. Yu, C. Yu, F. Guo, J. Wang, S. Jiao, S. Gao, H. Li and L. Zhao, *Energy Environ. Sci.*, 2012, **5**, 6151–6155.
38 F. Cao, G. Oskam and P. C. Searson, *J. Phys. Chem.*, 1995, **99**, 17071–17073.
39 J. Wu, S. Hao, Z. Lan, J. Lin, M. Huang, Y. Huang, L. Fang, S. Yin and T. Sato, *Adv. Funct. Mater.*, 2007, **17**, 2645–2652.
40 J. Wu, Z. Lan, J. Lin, M. Huang, S. Hao, T. Sato and S. Yin, *Adv. Mater.*, 2007, **19**, 4006–4011.
41 J. Wu, Z. Lan, J. Lin, M. Huang, Y. Huang, L. Fan and G. Luo, *Chem. Rev.*, 2015, **115**, 2136–2173.
42 Z. Yu, Q. Zhang, D. Qin, Y. Luo, D. Li, Q. Shen, T. Toyoda and Q. Meng, *Electrochem. Commun.*, 2010, **12**, 1776–1779.
43 H.-Y. Chen, L. Lin, X.-Y. Yu, K.-Q. Qiu, X.-Y. Lü, D.-B. Kuang and C.-Y. Su, *Electrochim. Acta*, 2013, **92**, 117–123.
44 S. Wang, Q.-X. Zhang, Y.-Z. Xu, D.-M. Li, Y.-H. Luo and Q.-B. Meng, *J. Power Sources*, 2013, **224**, 152–157.
45 K. Meng and K. R. Thampi, *ACS Appl. Mater. Interfaces*, 2014, **6**, 20768–20775.
46 H. Kim, I. HWang and K. Yong, *ACS Appl. Mater. Interfaces*, 2014, **6**, 11245–11253.
47 J. Duan, Q. Tang, Y. Sun, B. He and H. Chen, *RSC Adv.*, 2014, **4**, 60478–60483.
48 Y. Yang and W. Wang, *J. Power Sources*, 2015, **285**, 70–75.
49 Y. Yu, R. Peng, C. Yang and Y. Tang, *J. Mater. Sci.*, 2015, **50**, 5799–5808.
50 A. Panáček, R. Prucek, J. Hrbáč, T. Nevečná, J. šteffková, R. Zbořil and L. Kvítek, *Chem. Mater.*, 2014, **26**, 1332–1339.
51 W. Zhuang, L. Li and C. Liu, *SpringerPlus*, 2013, **2**, S11.
52 B.-Q. Lu, Y.-J. Zhu, X.-Y. Zhao, G.-F. Cheng and Y.-J. Ruan, *Mater. Res. Bull.*, 2013, **48**, 895–900.
53 F. Hua, *J. Mater. Sci.*, 2001, **36**, 731–738.
54 X. Zhong, Y. Feng and Y. Zhang, *J. Phys. Chem. C*, 2007, **111**, 526–531.
55 L. Liao, H. Zhang and X. Zhong, *J. Lumin.*, 2011, **131**, 322–327.
56 W. Li and X. Zhong, *J. Phys. Chem. Lett.*, 2015, **6**, 796–806.

57 Z. Pan, K. Zhao, J. Wang, H. Zhang, Y. Feng and X. Zhong, *ACS Nano*, 2013, **7**, 5215–5222.
58 Z. Du, H. Zhang, H. Bao and X. Zhong, *J. Mater. Chem. A*, 2014, **2**, 13033–13040.
59 K. Zhao, Z. Pan, I. Mora-Seró, E. Canovas, H. Wang, Y. Song, X. Gong, J. Wang, M. Bonn, J. Bisquert and X. Zhong, *J. Am. Chem. Soc.*, 2015, **137**, 5602–5609.
60 H. Zhang, H. Bao and X. Zhong, *J. Mater. Chem. A*, 2015, **3**, 6557–6564.
61 H. Kataoka, Y. Saito, Y. Uetani, S. Murata and K. Kii, *J. Phys. Chem. B*, 2002, **106**, 12084–12087.
62 G. Y. Gu, S. Bouvier, C. Wu, R. Laura, M. Rzeznik and K. M. Abraham, *Electrochim. Acta*, 2000, **45**, 3127–3139.
63 V. González-Pedro, X. Xu, I. Mora-Seró and J. Bisquert, *ACS Nano*, 2010, **4**, 5783–5790.

